Strong-field induced fragmentation and isomerization of toluene probed by ultrafast femtosecond electron diffraction and mass spectrometry

– Supporting Information–

Yanwei Xiong[1], Kurtis Borne[2], Andrés Moreno Carrascosa[3], Sajib Kumar Saha[1], Kyle J. Wilkin[1], Mengqi Yang[4] ,Surjendu Bhattacharyya[2] , Keyu Chen[2], Wenpeng Du[3], Lingyu Ma[3] , Nathan Marshall[2] , J. Pedro F. Nunes[1], Shashank Pathak[2], Zane Phelps[2], Xuan Xu[3], Haiwang Yong[3], Kenneth Lopata[4], Peter M. Weber[3], Artem Rudenko[2], Daniel Rolles[2], Martin Centurion[1]

[1]*University of Nebraska – Lincoln, Lincoln Nebraska, USA*

[2]*Kansas State University – Manhattan, Kansas, USA*

[3]*Brown University - Providence, Rhode Island, USA*

[4]*Louisiana State University, Baton Rouge, Louisiana, USA*

S1 Cation yields and laser intensity distribution

Here we describe the differences in the focal geometry of the TOF mass spectrometry and UED experiments, and how that might influence the measurements. The main difference is that the TOF measurement involves a single pulse, the laser, and ions are collected from the whole focal volume. In the UED experiment, the electron beam crosses the laser focus at an angle, thus, only the part of the laser focal volume is sampled by the electron beam. In our case, the electron beam is smaller than the laser beam, so the electrons preferentially sample molecules in the higher intensity region of the laser focus. Assume $P(k, I)$ is the probability of one cation k created from one toluene molecule per laser pulse with an uniform intensity I, and $\rho(I)dI$ is the number of molecules ionized by the laser field over the intensity range dI. The number of cations k generated is $dN(k,I) = P(k,I)\rho(I)dI$. Here $\rho(I)$ is the number density of molecules illuminated by laser intensity I. The molecule number density can be numerically calculated according to the interaction geometry. Integration of the equation over all laser intensities gives the total number of cations k, $N(k) = \int P(k,I)\rho(I)dI$. The relative abundance of cation k is $N(k) \Big/ \sum_i N(i)$.

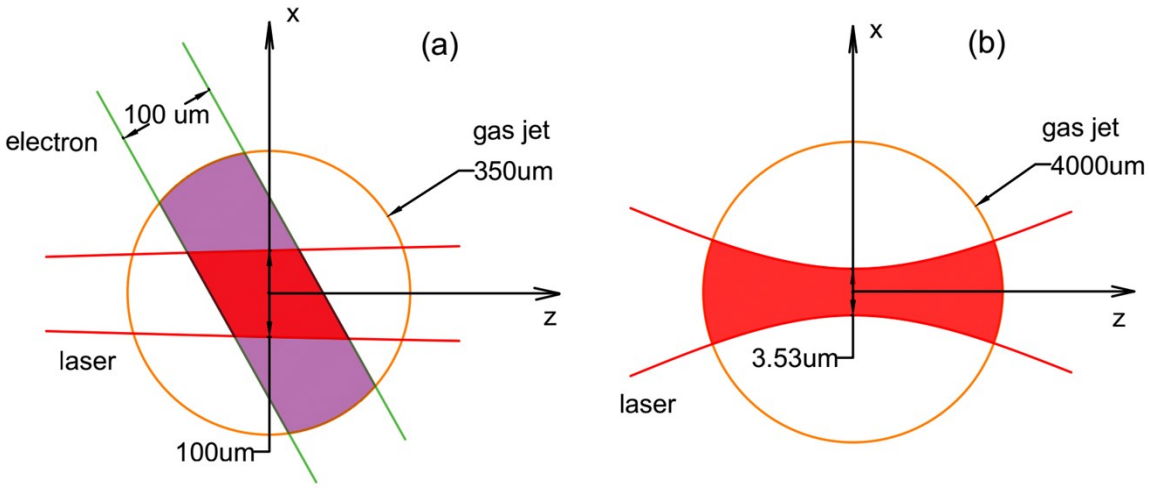

Figure S-1. (a) geometry of laser, electron beam and gas jet in UED experiment; (b) laser and gas jet in TOF

For the UED experiment, the diameter of the beams in the interaction region in full width at half maximum (FWHM) is 350 μm for the gas jet, 100 um×170 μm for the laser beam and 100 μm for the electron beam. In this setup the laser focus (20 μm FWHM) is 5 mm in front of the interaction region. The Rayleigh length is 1.13 mm, and the gas jet is 5 mm away from the laser focus. The laser beam diameter is approximated as constant over the width of the gas jet. The laser intensity in the gas jet can be written as

$$I_{laser\_UED}(x,y) = I_0 e^{-(\frac{x^2}{2c_x^2}+\frac{y^2}{2c_y^2})} \quad \text{(S-1a)}$$

The pulse energy E is equal to the integration of $I_{laser\_UED}(x,y)e^{-\frac{t^2}{2c_t^2}}$ over both time and space. Here $I_0 = \frac{E}{(2\pi)^{3/2}c_x c_y c_t} = 116TW/cm^2$, based on measurements of pulse duration, energy and spot size. The intensity of the electron beam and gas jet can be written as

$$I_{e\_UED} = \frac{1}{2\pi c_e^2} e^{-\frac{\left(\frac{1}{2}x+\frac{\sqrt{3}}{2}z\right)^2+y^2}{2c_e^2}} \quad \text{(S-1b)}$$

$$I_{gas\_UED} = \frac{1}{2\pi c_g^2} e^{-(\frac{x^2+z^2}{2c_g^2})} \quad \text{(S-1c)}$$

The percentage of molecules that contribute to the diffraction signal and are pumped by a certain laser intensity is determined by the overlap of the electron beam and gas jet. The $1/e^2$ width of the electron beam and gas jet are used to determine the overlap region. The laser intensity range from I_L to I_0 is considered in the numerical calculation, with the assumption that the relative yield of cations generated below laser

intensity I_L is negligible. Here we assume I_L=1 TW/cm^2. The molecule number density $\rho(I)$ is calculated using $\rho(I)= \Delta n/\Delta I$, where Δn is the number of molecules in the spatial region corresponding to laser intensity between I and $I+\Delta I$. The cumulative number of molecules $n(I)$ and density $\rho(I)$ is shown in figure S-2. $n(I)$ represents the number of molecules illuminated by an intensity larger than I.

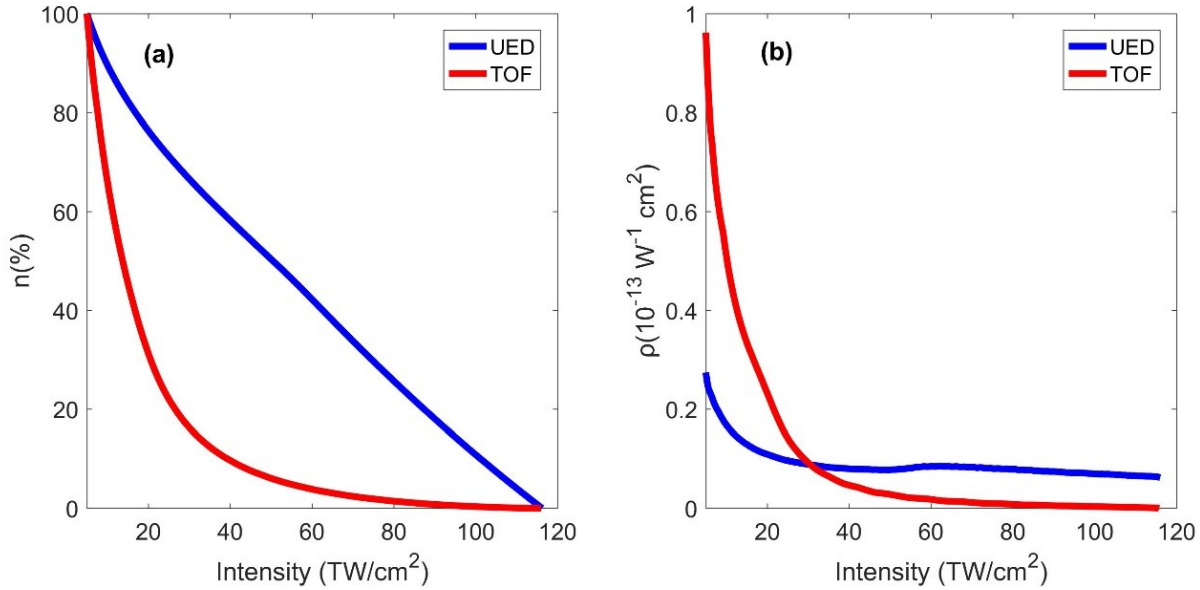

Figure S-2. UED (blue), TOF (red); (a) molecule number cumulative distribution $n(I)$ with total number normalized to 1. (b)the molecule number density $\rho(I) = -dn/dI$

For the TOF mass spectra measurement, the diameter of the gas jet (FWHM) is 4000 μm, the diameter of laser focus (FWHM) 3.53 μm , and Rayleigh length is 10 μm , see figure S-1(b). The laser intensity can be written as

$$I_{laser\_TOF} = I_0\left(\frac{w_0}{w(z)}\right)^2 e^{\frac{-2(x^2+y^2)}{w(z)^2}} \tag{S-2a}$$

where $w(z) = w_0\sqrt{1+(\frac{z}{z_R})^2}$, waist radius w_0=1.5 μm, and Rayleigh length $z_R = \frac{\pi w_0^2}{\lambda}$. The gas jet can be expressed as equation (S-1c) with a different c_g=4000 μm. The 1/e^2 width of the gas jet and the laser intensity ranging from 1TW/cm^2 to I_0 are used to calculate the n(I) and $\rho(I)$, shown in figure S-2. The comparison, assuming the same peak intensity in both cases, shows that the UED measurement will sample more molecules at higher intensities, relative to the TOF measurement.

S2 UED data analysis and fitting

Here we describe the steps for processing the UED experimental data.

(a) Image cleanup and normalization: The region of the image blocked by the beam stop is removed from the analysis. Outlier pixels are removed from each image. Each image is normalized to the average value of data within 60×60 pixels around s=2.4A^{-1}.

(b) Difference diffraction signal: The average diffraction pattern of 100 images (each with 1 min. acquisition time) is computed for each of the time delays: -5ps, 5ps, 10ps and 15ps. The diffraction difference pattern are calculated by taking the difference of the combined images for time delays at 5ps, 10ps and 15ps with the reference at -5ps, $\Delta I_{2d}(s,t) = I_{2d}(s,t) - I_{2d}(s,t_{ref} = -5ps)$.

(c) Azimuthal averaging: We applied Legendre projection [1] to the 2-dimensional diffraction difference pattern to obtain the isotropic component, and then azimuthally averaged the 2-dimensional diffraction difference pattern to calculate 1-dimensional diffraction difference signal $\Delta I_{exp}(s,t)$ and corresponding standard errors for each s as $\sigma(s,t)$. The modified diffraction difference intensity is calculated by $\Delta sM_{exp} = \frac{s\Delta I_{exp}}{I_{at\_tol}}$, shown in figure S-3, where I_{at_tol} is the simulated atomic scattering of toluene.

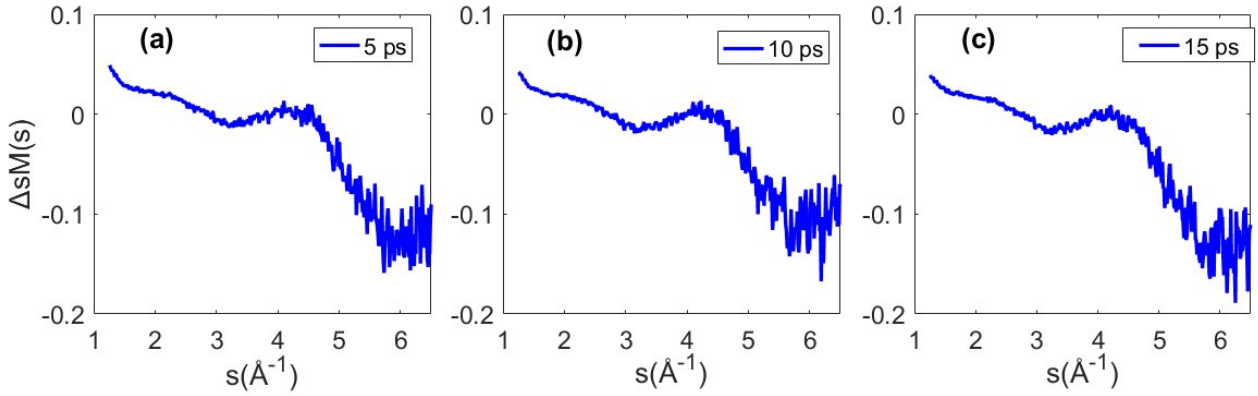

Figure S-3. (a-c) ΔsM_{exp} for different time delays using reference time t_{ref}=-5ps.

(d) Background correction: The modified diffraction signals have a residual background. To obtain the abundance of fragment pairs from the experimental modified diffraction signal $\Delta sM_{exp}(s)$, we first remove the residual background with the method [2] used to fit the residual background for static diffraction. We construct a function with the simulated ΔsM (labeled as $y_j(s)$ in the following equation) from each fragment pair and a set of parameters, $\Delta sM_T(s,c_j) = \sum_{j=1}^{k} c_j y_j(s)$. The values of experimental data at the zero positions of $\Delta sM_t(s,c_j)$ are used to fit a background $b(s,c_j)$ with a 2nd order polynomial. The set of coefficients c_j with the constraint $\sum_{j=1}^{k} c_j = ef$ (ef indicates the percentage of toluene ionization) that minimizes the equation $\chi^2(c_1,c_2,\ldots,c_k) = \frac{1}{N-k}\sum_{x=1}^{N}\left(\frac{Y(x) - b(x,c_j) - Y_T(x,c_j)}{\sigma(x)}\right)^2$ gives the yield of each fragment pair.

(e) Fitting: We used an iterative method to find the local minimum of χ^2. Assume the initial coefficients for each component are $(p_1^1,p_2^1,\ldots,p_k^1)$, we construct the scan range for each coefficient c_j by adding and subtracting a small value δ_j, $(p_j^1-\delta_j,p_j^1,p_j^1+\delta_j)$. Therefore, there are 3^k sets of coefficients, one of which gives the minimum value of χ^2, for example $(p_1^1,p_2^1-\delta_2,\ldots,p_k^1+\delta_k)$, will be used as the new coefficients $(p_1^2,p_2^2,\ldots,p_k^2)$ for the next iteration. Each iteration follows the gradient of the χ^2 and provides a smaller χ^2. The calculation iterates many times until $\chi^2(p_1^m,p_2^m,\ldots,p_k^m)$ is no more than $\chi^2(p^{m+1}_1,p^{m+1}_2,\ldots,p^{m+1}_k)$. The iterations adjust the coefficients automatically to approach a smaller χ^2 each time until the minimum is found.

(f) Fitting results and standard error: Bootstrapping is used to obtain the standard error of the fitted parameters. 100 images are randomly selected out of the 100 images for each time delay to calculate the $\Delta sM_{exp}(s)$, followed by the parameters fitting, to obtain the parameter and confidence interval of each component. The simulated sM of the most prevalent cations ($C_4H_4^+$,$C_3H_4^+$), ($C_6H_5^+$,CH_3^+), ($C_5H_3^+$,$C_2H_3^+$), Tr^+, Bz^+ and Tol^+, are chosen to do the fitting for the $\Delta sM_{exp}(s)$. Figure S-4 shows the fitted results of the modified diffraction-difference signal ΔsM at time delays of 5 ps, 10 ps and 15 ps. The combined data set, i.e. the average of the 3 different time delays, is fitted to obtain the normalization constant (ef in Table S-1), which corresponds to the percentage of ionized molecules within the interaction volume. The parameters and the confidence intervals using the bootstrapping approach are shown in table S-1. The fragment yields at different time delays are shown in figure S-5. There is some indication that some fragment yields might increase after 5 ps, although further study is needed to reduce the uncertainties to address this point. Overall the fragment yields observed at different times are in agreement within the measurement uncertainties. The results of the fit are comparable when using different fragment pairs form each group to do the fit. The yields obtained from fitting using the second most prevalent cations ($C_4H_3^+$,$C_3H_5^+$), ($C_6H_5^+$,CH_3), ($C_5H_5^+$,$C_2H_3^+$), Tr^+, Bz^+ and Tol^+ cations is shown in figure S-6, which shows similar results. The results are not very sensitive to the number of hydrogen atoms in each fragment.

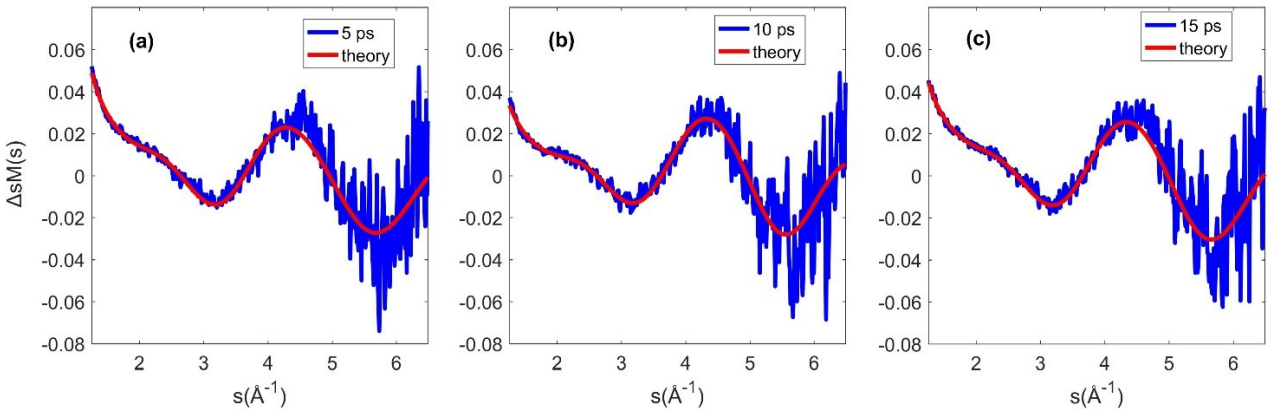

Figure S-4. ΔsM fit for time delay: (a) 5ps, (b)10ps, (c)15ps. experimental ΔsM (blue); theoretical ΔsM (red).

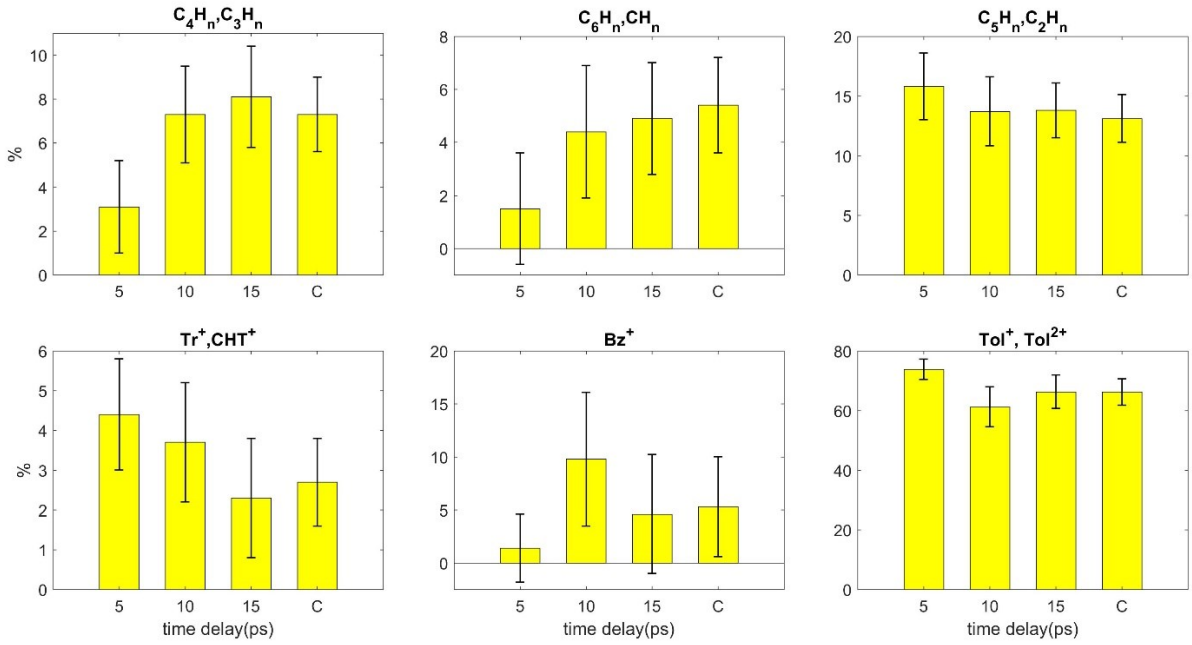

Figure S-5. Cation yields using the fragment pairs ($C_4H_4^+$,$C_3H_4^+$), ($C_6H_5^+$,CH_3^+), ($C_5H_3^+$,$C_2H_3^+$), Tr^+, Bz^+ and Tol^+ cations. The last bar in each plot is the cation yield fitted with combined dataset.

Table S-1. Fitted abundance of the experimental ΔsM. The last row (C) is fitted parameters with the combined data at 3 different time delays after time zero.

%	C_4H_m,C_3H_n	C_6H_m,CH_n	C_5H_m,C_2H_n	Tr^+, CHT^+	Bz^+	Tol^+	ef	χ^2
5ps	3.13±2.14	1.48±2.08	15.77±2.79	4.41±1.41	1.44±3.17	73.78±3.41	0.12	1.88±0.09
10ps	7.26±2.19	4.37±2.51	13.73±2.91	3.70±1.45	9.78±6.34	61.18±6.70	0.12	1.85±0.11
15ps	8.09±2.31	4.95±2.15	13.79±2.34	2.29±1.47	4.63±5.63	66.27±5.58	0.12	1.82±0.09
C	7.30±1.71	5.40±1.82	13.14±2.01	2.66±1.15	5.31±4.68	66.20±4.44	0.12	1.88±0.08

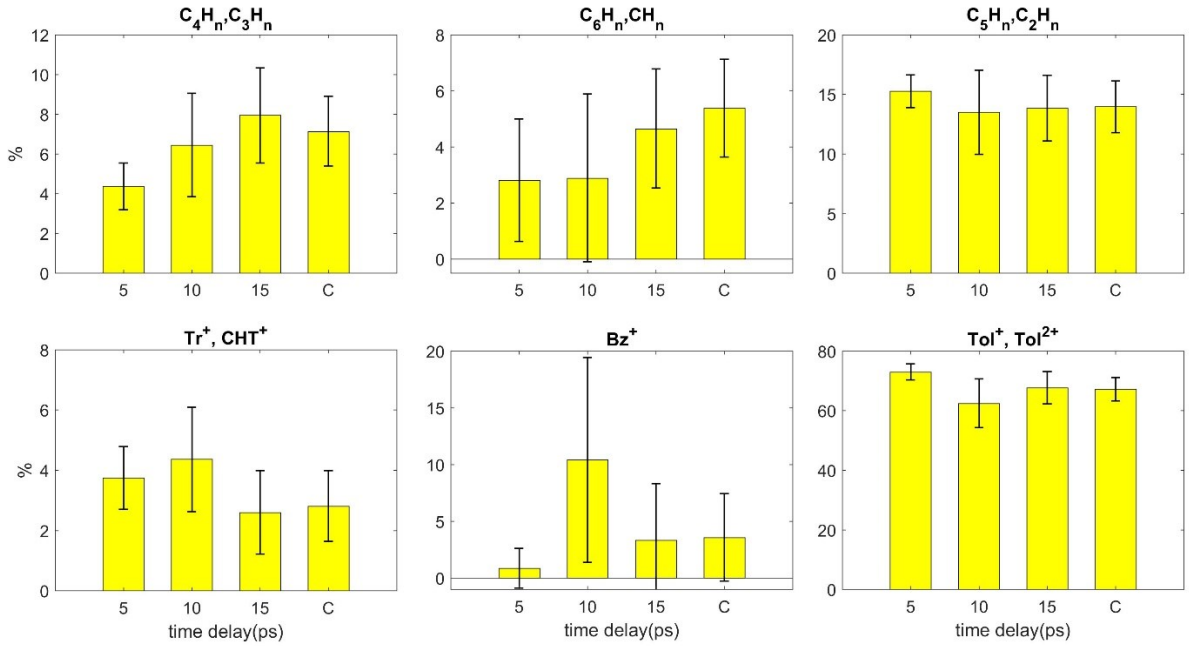

Figure S-6. Cations yields using the fragment pairs ($C_4H_3^+$,$C_3H_5^+$), ($C_6H_5^+$,CH_3), ($C_5H_5^+$,$C_2H_3^+$), Tr^+, Bz^+ and Tol^+ cations. The last bar in each plot is the cation yield fitted with combined data at three different time delays after time zero.

S3 Simulated ΔsM using the independent atomic model (IAM)

Here we calculate the ΔsM of the fragment pairs using the IAM for the comparison with the ab-initio scattering calculations (Figure S-7). We use the geometry optimized (section 4.2 main text) with CASSCF level of theory (table 4 in the main text).

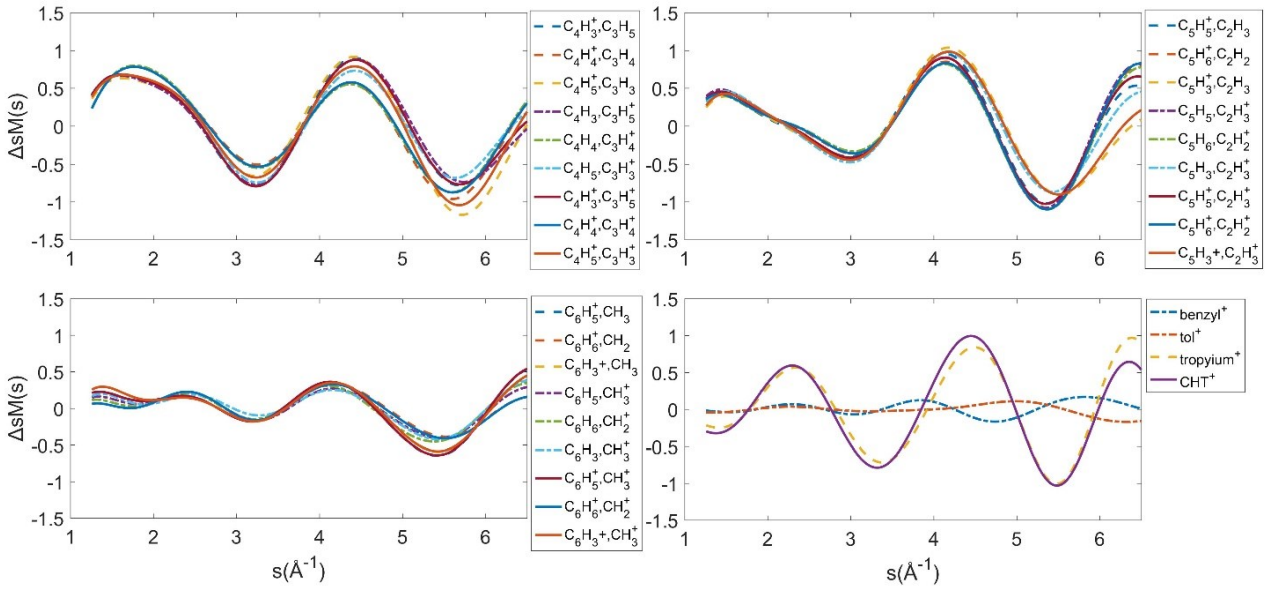

Figure S-7. Simulated ΔsM for fragments pairs using diffraction theory based on the independent atomic model

Reference

1. Baskin, J.S. and A.H. Zewail, *Oriented ensembles in ultrafast electron diffraction.* Chemphyschem, 2006. **7**(7): p. 1562-74.
2. Ihee, H., et al., *Ultrafast Electron Diffraction and Structural Dynamics: Transient Intermediates in the Elimination Reaction of C2F4I2.* The Journal of Physical Chemistry A, 2002. **106**(16): p. 4087-4103.